

Resolving the Solar Neutrino Problem with KamLAND

V. Barger, Danny Marfatia and Benjamin P. Wood
Department of Physics, University of Wisconsin-Madison, WI 53706

Abstract

We study how well KamLAND, the first terrestrial neutrino experiment capable of addressing the solar neutrino problem, will perform in ascertaining whether or not the large mixing angle MSW solution (with $10^{-5} \lesssim \Delta m_{21}^2 \lesssim 10^{-4} \text{ eV}^2$ and oscillation amplitude $\sin^2 2\theta_{12} > 0.3$) is correct. We find that in a year of operation KamLAND will provide unequivocal evidence for or against this solution. Furthermore, its sensitivity to the three-neutrino oscillation parameters in this region is sufficiently acute as to determine Δm_{21}^2 to approximately $\pm 10\%$ (for $\sin^2 2\theta_{12} > 0.7$) and to fix $\sin^2 2\theta_{12}$ to within ± 0.1 (at the 2σ level) with three years of accumulated data, independent of the value of θ_{13} .

I. INTRODUCTION

Several neutrino oscillation experiments now indicate that neutrinos are massive and that neutrino flavor mixing occurs. Atmospheric neutrino experiments (Kamiokande [1], SuperKamiokande [2], IMB [3], Soudan [4] and MACRO [5]) report a ν_μ/ν_e event ratio that is about 0.6 times the expected ratio; the ν_μ flux shows a zenith angle dependence that is explained by oscillations. All experiments that measure the solar neutrino flux (Homestake [6], SAGE [7], GALLEX [8], Kamiokande [9] and SuperKamiokande [10]) find a deficit of 1/2 to 1/3 of the Standard Solar Model prediction [11]. LSND [12], an accelerator experiment, finds evidence for $\bar{\nu}_\mu \rightarrow \bar{\nu}_e$ and $\nu_\mu \rightarrow \nu_e$ oscillations, a result that is not excluded by KARMEN [13] and awaits confirmation by MiniBooNE [14]. The current generation of nuclear reactor experiments (Palo Verde [15] and CHOOZ [16]) find null oscillation results and rule out $\bar{\nu}_e \rightarrow \bar{\nu}_x$ oscillations for $\Delta m_{21}^2 \gtrsim 10^{-3} \text{ eV}^2$ at maximal mixing and $\sin^2 2\theta_{13} > 0.1$ for larger Δm_{21}^2 (at the 95% confidence level).

The focus of the present work is the solar neutrino puzzle [17] and KamLAND's [18] role in resolving whether or not the large mixing angle (LMA) solution (see *e.g.* Ref. [19]) is the correct one. The LMA solution has Δm_{21}^2 in the range 10^{-5} to 10^{-4} eV^2 and mixing amplitude $\sin^2 2\theta_{12} > 0.3$. Data from SuperKamiokande [20] now favors the LMA solution over the small mixing angle, low and vacuum oscillation solutions (see Ref. [21] for a discussion of the various oscillation solutions). Solar neutrino measurements at SNO [22] should discriminate between different oscillation solutions, but perhaps not in its first year of operation [23]. If the LMA solution is the correct one, KamLAND will provide a precise determination of the oscillation parameters.

KamLAND is unique in its potential as the first terrestrial experiment to explore the solar neutrino anomaly. It will provide a definitive test of the LMA solution by either ruling it out or by pinning down the values of Δm_{21}^2 and $\sin^2 2\theta_{12}$. KamLAND should be able to provide this answer in a year from the start of running in spring 2001 and then provide an accurate determination of the solar neutrino oscillation parameters by the end of the three years over which it is expected to take data for. Particularly significant will be its ability to precisely determine Δm_{21}^2 in the LMA region because unlike the case of solar neutrinos, the Δm_{21}^2 -dependent contribution to oscillations of the reactor neutrinos will not suffer from averaging of the oscillation L/E dependence.

If the LMA solution is correct, Δm_{21}^2 -dependent CP -violating effects [24] can be large enough to be tested at very long baseline accelerator-based experiments [25]. With KamLAND promising a precisely known value of Δm_{21}^2 , it will provide essential information for future experiments studying CP -violation in the neutrino sector.

In Section II we provide a brief overview of the KamLAND experiment and the oscillation hypothesis in which we will work. Section III will be devoted to details of our simulation of the experiment and the subsequent data analysis. We conclude in Section IV.

II. THE KAMLAND EXPERIMENT

KamLAND is a reactor neutrino experiment with its detector located at the Kamiokande site. With low energy neutrinos ($\langle E_\nu \rangle \sim 3 \text{ MeV}$), it can only measure $\bar{\nu}_e$ disappearance and therefore will be unable to access small mixing angles $\sin^2 2\theta_{12} < 0.1$. About 95% of the $\bar{\nu}_e$

flux incident at KamLAND will be from reactors situated between 80 – 350 km from the detector, making the baseline long enough to provide a sensitive probe of the LMA solution of the solar neutrino problem. Specifically, the sensitivity to the mass-squared differences will lie between $\Delta m_{21}^2 \sim (L(\text{m})/E(\text{MeV}))^{-1} \gtrsim 10^{-5} \text{ eV}^2$ and $\lesssim 10^{-4} \text{ eV}^2$. Despite the absence of a single baseline, the measured positron energy spectrum allows a sensitive probe of oscillation effects.

We consider a framework of three-flavor oscillations among the massive neutrinos (ν_1, ν_2, ν_3) . In the phenomenologically interesting limit, $\Delta m^2 \equiv m_2^2 - m_1^2 \ll m_3^2 - m_2^2$, the survival probability at the detector is given by

$$P(\bar{\nu}_e \rightarrow \bar{\nu}_e) = 1 - 2 s_{13}^2 c_{13}^2 - 4 s_{12}^2 c_{12}^2 c_{13}^4 \sin^2 \left(\frac{1.27 \Delta m^2 (\text{eV}^2) L(\text{m})}{E_\nu (\text{MeV})} \right), \quad (1)$$

where $s_{ij}^2 = 1 - c_{ij}^2 = \sin^2 \theta_{ij}$ are the neutrino mixing parameters, L is the distance of the detector from the source and E_ν is the energy of the anti-neutrino. Here we have averaged over the leading oscillations $\langle \sin^2(1.27 |m_3^2 - m_2^2| L/E_\nu) \rangle = 1/2$. Matter effects on oscillations are negligible at the KamLAND baseline.

Although we restrict our analysis to three neutrino oscillations, it is possible that the transition $\bar{\nu}_e \rightarrow \bar{\nu}_s$, where ν_s is a sterile neutrino, is responsible for the depletion of the $\bar{\nu}_e$ flux. (See Refs. [26,27] for models and analyses of four-neutrino oscillations for the solar and atmospheric anomalies). For example, in a $2 + 2$ neutrino mixing scheme, in which one pair of nearly degenerate mass eigenstates has maximal $\nu_e \rightarrow \nu_s$ mixing for solar neutrinos and the other pair has nearly maximal mixing $\nu_\mu \rightarrow \nu_\tau$ for atmospheric neutrinos, the survival probability is [26]

$$P(\bar{\nu}_e \rightarrow \bar{\nu}_e) = 1 - 4 \epsilon^2 - \sin^2 \left(\frac{1.27 \Delta m^2 (\text{eV}^2) L(\text{m})}{E_\nu (\text{MeV})} \right), \quad (2)$$

where $\epsilon \simeq (0.016 \text{ eV}^2 / \Delta m_{LSND}^2)^{0.91}$ is restricted by KARMEN [13] and BUGEY [28] to be in the interval (0.01, 0.1) corresponding to a Δm_{LSND}^2 range 0.2 to 1.7 eV^2 [26]. In Eq. (2) we have averaged over the leading oscillations associated with the LSND mass scale. On comparing Eq. (1) (fixing $\theta_{12} = \pi/4$ and $\sin^2 2\theta_{13} = 0.1$) with Eq. (2), one sees that KamLAND will be unable to distinguish whether the oscillations are to flavor or to sterile neutrinos, but neutral current measurements at SNO will accomplish this. KamLAND is more sensitive to θ_{13} than to ϵ , and we find that it will not provide useful information about θ_{13} and consequently even less about ϵ . In the following, we base our analysis on Eq. (1).

The target for the $\bar{\nu}_e$ flux consists of a spherical transparent balloon filled with 1000 tons of non-doped liquid scintillator. The anti-neutrinos are detected via the inverse neutron β -decay

$$\bar{\nu}_e + p \rightarrow e^+ + n. \quad (3)$$

The cross section for this process is [29]

$$\begin{aligned} \sigma(E_\nu) &= \frac{2 \pi^2}{m_e^5 f \tau_n} (E_\nu - \Delta M) [(E_\nu - \Delta M)^2 - m_e^2] \\ &= 0.952 \frac{(E_\nu - \Delta M) [(E_\nu - \Delta M)^2 - m_e^2]}{1 \text{ MeV}^2} \times 10^{-43} \text{ cm}^2, \end{aligned} \quad (4)$$

Reactor	Distance (km)	Percent of total flux
Kashiwazaki	160.0	33.36
Ohi	179.5	14.76
Takahama	190.6	9.76
Shiga	80.6	8.51
Tsuruga	138.6	8.12
Mihama	145.4	8.10
Hamaoka	214.0	8.06
Fukushima – 1	344.0	4.17
Fukushima – 2	344.0	3.86
Tokai – II	294.6	1.30

TABLE I. The expected relative contribution of each reactor to the $\bar{\nu}_e$ flux detected at KamLAND in the case of no oscillations. Only reactors in a 350 km radius of the detector are considered.

where m_e is the mass of the electron, $\Delta M = m_n - m_p$ is the neutron-proton mass difference, $\tau_n = (886.7 \pm 1.9)$ s is the neutron lifetime and $f = 1.7152$ is the phase space factor which includes Coulomb, weak magnetism, recoil and outer radiative corrections. The theoretical error in the above cross section is less than a percent. The neutrino capture process has a threshold of $\Delta M + m_e = 1.804$ MeV and the $\bar{\nu}_e$ flux above this threshold is 1.3×10^6 cm⁻² s⁻¹ which is known to a precision of about 1.4% [30]. In the case of no oscillations, KamLAND expects to see ~ 800 events per year with a background ~ 40 events per year. The distribution of the background events versus positron energy is expected to be known, thus facilitating a clean extraction of the signal. We will assume that a background subtraction can be made for our data simulation and analysis.

III. DATA SIMULATION AND ANALYSIS

To calculate the $\bar{\nu}_e$ flux we include contributions from all nuclear reactors within a radius of 350 km from the detector. Table I gives the relative fluxes (without oscillations) and thus shows the relative importance of each reactor to the experiment (total fluxes from each reactor are tabulated in Ref. [18]). The $\bar{\nu}_e$ spectrum above the 1.8 MeV threshold for the process (3) is the result of the decay of fission fragments of the isotopes ²³⁵U, ²³⁹Pu, ²³⁸U and ²⁴¹Pu. The spectrum from the fission products of each of these isotopes can be found in [31]. As the reactor operates, the concentration of ²³⁵U decreases and that of ²³⁹Pu and ²⁴¹Pu increases. We do not account for the fissile isotope evolution and instead assume a typical fraction of fissions (as in Ref. [30]) from the four fissile materials (see Table II). We have confirmed that the effect of the evolution is small by reproducing the $\bar{\nu}_e$ spectrum from the Palo Verde experiment [15].

With the relative flux from each reactor known, and the knowledge of the $\bar{\nu}_e$ spectrum (assumed to be the same for all reactors), we calculated the e^+ spectrum at KamLAND resulting from inverse β -decay and normalized it to yield a total of 800 events per year in the absence of oscillations. This procedure effectively accounts for the effective number of free protons in the target, the e^+ and n efficiencies, the efficiency of the $e^+ - n$ distance cut

	Start of Cycle (%)	End of Cycle (%)	Typical value (%)
^{235}U	60.5	45.0	53.8
^{239}Pu	27.2	38.8	32.8
^{238}U	7.7	8.3	7.8
^{241}Pu	4.6	7.9	5.6

TABLE II. The fraction of fissions from the four fissile elements in a nuclear reactor at the beginning of the cycle, the end of the cycle and a typical value during a cycle taken from Ref. [30].

and fluctuations in the power output of the reactors arising from dead time for maintenance and seasonal variations of power requirements.

Figure 1 shows the e^+ energy spectrum expected at KamLAND with three years of data, illustrated for the cases of no oscillations (dotted histogram) and $(\Delta m^2, \sin^2 2\theta_{12}) = (7 \times 10^{-5} \text{ eV}^2, 0.75)$ (solid histogram). Each simulated data point is generated by randomly choosing a point from a Gaussian distribution centered at the theoretical value and of width equal to the square root of the theoretical value. The lower plot shows the ratio of the simulated data to the expectation for no oscillations. The errors shown are statistical. The plots are versus the total e^+ energy. A plot of the total measurable energy would be shifted to the right by $m_e = 0.511 \text{ MeV}$ because the $\bar{\nu}_e$ signature involves a measurement of the kinetic energy of the e^+ and the annihilation energy in the form of two 0.511 MeV gamma rays. Figure 2 illustrates the significant changes in the e^+ spectrum for different values of Δm^2 at a given value of $\sin^2 2\theta_{12}$. The spectra overlap to a large extent for values of $\Delta m^2 \gtrsim 2 \times 10^{-4} \text{ eV}^2$.

For the statistical analysis we define χ^2 as

$$\chi^2(\Delta m^2, \sin^2 2\theta_{12}) = \sum_{i=1}^{17} \frac{(N_{\text{simulated}}(E_i) - N(E_i, \Delta m^2, \sin^2 2\theta_{12}))^2}{N_{\text{simulated}}(E_i)}, \quad (5)$$

where i labels the 17 e^+ energy bins each of width 0.4 MeV and midpoint E_i , $N_{\text{simulated}}(E_i)$ is the number of simulated events in the i^{th} bin and $N(E_i, \Delta m^2, \sin^2 2\theta_{12})$ is the corresponding theoretical value for oscillation parameters $(\Delta m^2, \sin^2 2\theta_{12})$. The only fitted parameters are Δm^2 and $\sin^2 2\theta_{12}$. We keep $\sin^2 2\theta_{13}$ fixed when performing the χ^2 analysis (using the Levenberg-Marquadt method). From CHOOZ we know that $\sin^2 2\theta_{13} < 0.1$ and we consider the two extreme cases $\sin^2 2\theta_{13} = 0$ and $\sin^2 2\theta_{13} = 0.1$.

It is important to note that the main source of uncertainty in the experiment comes from conversion of the fission rates in the reactors to $\bar{\nu}_e$ fluxes and the normalization uncertainty is expected to be less than 3% [32]. (The CHOOZ experiment [16] had a normalization uncertainty of 2.7%). Even if the combined systematic uncertainty could be as large as 5%, the shapes and sizes of the confidence contours in our analysis would be unaffected by its inclusion. We can thus safely ignore systematic uncertainties in what follows.

We concentrate on the region defined by $\sin^2 2\theta_{12} > 0.2$ and $10^{-5} < \Delta m^2 < 2 \times 10^{-4} \text{ eV}^2$. For values of Δm^2 outside this region, sensitivity to the neutrino energy-dependence is lost. For $\Delta m^2 \lesssim 10^{-5} \text{ eV}^2$, the value of the oscillation-dependent sinusoidal factor gets small. For $\Delta m^2 \gtrsim 2 \times 10^{-4} \text{ eV}^2$, the argument of the Δm^2 -dependent sine function in Eq. (1) becomes large because of the long baseline and the oscillations get averaged. By studying

the behavior of $\chi^2 - \chi_{min}^2$ as a function Δm^2 for several simulated datasets, we find that for theoretical inputs with $\Delta m_{theor}^2 \lesssim 2 \times 10^{-4} \text{ eV}^2$, $\chi^2 - \chi_{min}^2$ has unique, well-defined minima at the theoretical values. For inputs with $\Delta m_{theor}^2 \gtrsim 2 \times 10^{-4} \text{ eV}^2$ we find the presence of more than one acceptable minimum in the region $2 \times 10^{-4} \lesssim \Delta m^2 \lesssim 10^{-3} \text{ eV}^2$ [33] and a continuum of solutions $\Delta m^2 \gtrsim 10^{-3} \text{ eV}^2$ that are acceptable at the 2σ level. Thus, for values larger than $2 \times 10^{-4} \text{ eV}^2$, KamLAND can place a lower bound on Δm^2 , but cannot uniquely determine the value. However, the region of good sensitivity covers the entire LMA solution.

Figure 3 shows fits to e^+ spectra (expected after three years of running) for values of Δm^2 and $\sin^2 2\theta_{12}$ covering the entire region of the LMA solution with $\theta_{13} = 0$. The plot shows 1σ (68.3%) and 2σ (95.4%) confidence contours. The diamond is the theoretical value for which data was simulated and the cross marks the best fit point. Each point is labelled by the expected number of signal events. The χ^2 value for the best fit corresponds to a χ^2 probability of at least 80%. For a given value of Δm^2 , the confidence regions get flatter along the Δm^2 -direction as $\sin^2 2\theta_{12}$ is increased from 0.2 to 1, resulting in a finer determination of Δm^2 for larger $\sin^2 2\theta_{12}$. The value of $\sin^2 2\theta_{12}$ will be determined to an accuracy of ± 0.1 (2σ) throughout almost all of the parameter space under consideration. The Δm^2 value will be determined within $\pm 10\%$ (2σ) of its actual value for $10^{-5} \lesssim \Delta m^2 \lesssim 2 \times 10^{-4} \text{ eV}^2$ and $\sin^2 2\theta_{12} > 0.7$.

We found that for $\sin^2 2\theta_{13} = 0.1$ the contours are almost identical to that of Fig. 3; thus, KamLAND will not be sensitive to θ_{13} in any region of the parameter space. In Fig. 4 we show the expectation with one year of accumulated data (taking $\theta_{13} = 0$) and find that in this time period KamLAND should already give us the LMA parameters to reasonably good accuracy.

IV. CONCLUSION

The results of our work are succinctly summarized in Figs. 3–4. Within one year of operation, KamLAND measurements of the reactor $\bar{\nu}_e$ flux will establish whether or not the LMA solution ($10^{-5} \lesssim \Delta m_{21}^2 \lesssim 10^{-4} \text{ eV}^2$ and $\sin^2 2\theta_{12} > 0.3$) is correct. If it is, in a span of three years the accuracy with which $\sin^2 2\theta_{12}$, and especially Δm_{21}^2 , will be determined is striking. KamLAND will give us $\sin^2 2\theta_{12}$ to an accuracy of ± 0.1 and Δm_{21}^2 to within a factor of 2 for $\sin^2 2\theta_{12} > 0.2$; Δm_{21}^2 will be known to an accuracy of $\pm 10\%$ for $\sin^2 2\theta_{12} > 0.7$ (at the 2σ level). However, no knowledge will be gleaned about θ_{13} . Our conclusions assume that the experiment employs a 1000 ton fiducial volume. If the fiducial volume is instead 600 tons, Fig. 4 applies for data collected over 20 months instead of 12 and the contours of Fig. 3 will be roughly twice as large at the end of three years. Details of systematic uncertainties and the accuracy with which the background shape is known will cause minor changes in our results, but the overall conclusions will remain intact.

If the LMA solution is found to be correct, the precision with which Δm_{21}^2 will be pinned down at KamLAND will prove to be very beneficial to studies of CP -violation in the lepton sector in long baseline experiments [34,35].

ACKNOWLEDGMENTS

We thank A. Baldini, J. Learned and K. Whisnant for discussions. This work was supported in part by a DOE grant No. DE-FG02-95ER40896 and in part by the Wisconsin Alumni Research Foundation.

REFERENCES

- [1] K. Hirata *et al.*, Phys. Lett. **B205**, 416 (1988); Phys. Lett. **B280**, 146 (1992).
- [2] Y. Fukuda *et al.*, Phys. Lett. **B433**, 9 (1998); Phys. Rev. Lett. **81**, 1562 (1998); Phys. Rev. Lett. **82**, 2644 (1999); Phys. Lett. **B467**, 185 (1999).
- [3] D. Casper *et al.*, Phys. Rev. Lett. **66**, 2561 (1991); R. Becker-Szendy *et al.*, Phys. Rev. **D46**, 3720 (1992); Phys. Rev. Lett. **69**, 1010 (1992).
- [4] W. Allison *et al.*, Phys. Lett. **B391**, 491 (1997); Phys. Lett. **B449**, 137 (1999).
- [5] M. Ambrosio *et al.*, Phys. Lett. **B434**, 451 (1998); hep-ex/0001044.
- [6] B. Cleveland, T. Daily, R. Davis, Jr., J. Distel, K. Lande, C. Lee, P. Wildenhain and J. Ullman, Astropart. Phys. **496**, 505 (1998).
- [7] J. Abdurashitov *et al.*, Phys. Rev. **C60**, 055801 (1999).
- [8] W. Hampel *et al.*, Phys. Lett. **B447**, 127 (1999).
- [9] Y. Fukuda *et al.*, Phys. Rev. Lett. **77**, 1683 (1996).
- [10] Y. Fukuda *et al.*, Phys. Rev. Lett. **82**, 1810 (1999); Phys. Rev. Lett. **82**, 2430 (1999).
- [11] J. Bahcall, S. Basu and M. Pinsonneault, Phys. Lett. **B433**, 1 (1998).
- [12] C. Athanassopoulos *et al.*, Phys. Rev. Lett. **77**, 3082 (1996); Phys. Rev. Lett. **81**, 1774 (1998).
- [13] K. Eitel and B. Zeitnitz, Nucl. Phys. B (Proc. Suppl) **77**, 212 (1999).
- [14] A. Bazarko, hep-ex/0009056.
- [15] F. Boehm *et al.*, Phys. Rev. **D62**, 072002 (2000); Phys. Rev. Lett. **84**, 3764 (2000).
- [16] M. Apollonio *et al.*, Phys. Lett. **B466**, 415 (1999); Phys. Lett. **B420**, 397 (1998); D. Nicoló, PhD thesis, INFN, Pisa, Scuola Normale Superiore, (1999).
- [17] J. Bahcall, *Neutrino Astrophysics* (Cambridge University Press, Cambridge, England, 1989).
- [18] The KamLAND proposal, Stanford-HEP-98-03; A. Piepke, talk at *Neutrino-2000*, XIXth International Conference on Neutrino Physics and Astrophysics, Sudbury, Canada, June 2000.
- [19] G. Fogli, E. Lisi, D. Montanino and A. Palazzo, Phys. Rev. **D62**, 013002 (2000); M. Gonzalez-Garcia, M. Maltoni, C. Pena-Garay and J. Valle, hep-ph/0009350; J. Bahcall, P. Krastev and A. Yu. Smirnov, Phys. Rev. **D60**, 093001 (1999); N. Hata and P. Langacker, Phys. Rev. **D56**, 6107 (1997).
- [20] Y. Takeuchi, talk at *ICHEP2000*, XXXth International Conference on High Energy Physics, Osaka, Japan, July 2000.
- [21] J. Bahcall, P. Krastev and A. Yu. Smirnov, Phys. Rev. **D58**, 096016 (1998).
- [22] A. McDonald, Nucl. Phys. B (Proc. Suppl) **77**, 43 (1999); J. Boger *et al.* Nucl. Instrum. Meth. **A449**, 172 (2000).
- [23] J. Bahcall, P. Krastev and A. Yu. Smirnov, Phys. Lett. **B477**, 401 (2000).

- [24] V. Barger, K. Whisnant and R. Phillips, Phys. Rev. Lett. **45**, 2084 (1980); S. Pakvasa in *High Energy Physics–1980*, edited by L. Durand and L. Pondrom, AIP Conf. Proc. No. 68 (AIP, New York, 1981), p. 1164.
- [25] V. Barger, S. Geer, R. Raja and K. Whisnant, Phys. Rev. **D62**, 073002 (2000); A. Cervera, A. Donini, M. Gavela, J. Gomez Cadenas, P. Hernandez, O. Mena and S. Rigolin, Nucl. Phys. **B579** 17, (2000); A. De Rujula, M. Gavela and P. Hernandez, Nucl. Phys. **B547** 21, (1999); S. Bilenkii, C. Giunti and W. Grimus, Phys. Rev. **D58**, 033001 (1998); J. Arafune, M. Koike and J. Sato, Phys. Rev. **D56**, 3093 (1997); A. Bueno, M. Campanelli, A. Rubbia, Nucl. Phys. **B589** 577, (2000); I. Mocioiu and R. Shrock, Phys. Rev. **D62**, 053017 (2000).
- [26] V. Barger, B. Kayser, J. Learned, T. Weiler, K. Whisnant, Phys. Lett. **B489**, 345 (2000).
- [27] O. Peres, A. Yu. Smirnov, hep-ph/0011054; O. Yasuda, hep-ph/0006319; G. Fogli, E. Lisi and A. Marrone, hep-ph/0009299; C. Giunti, M. Gonzalez-Garcia, C. Pena-Garay, Phys. Rev. **D62**, 013005 (2000); D. Dooling, C. Giunti, K. Kang and C. Kim, Phys. Rev. **D61**, 073011 (2000). S. Bilenkii, C. Giunti, W. Grimus and T. Schwetz, Phys. Rev. **D60**, 073007 (1999).
- [28] Y. Declais *et al.*, Nucl. Phys. **B434** 503, (1995).
- [29] P. Vogel and J. Beacom, Phys. Rev. **D60**, 053003 (1999).
- [30] Y. Declais *et al.*, Phys. Lett. **B338**, 383 (1994).
- [31] K. Schreckenbach, G. Colvin, W. Gelletly and F. Von Feilitzsch, Phys. Lett. **B160**, 325 (1985); A.A. Hahn, K. Schreckenbach, G. Colvin, B. Krusche, W. Gelletly and F. Von Feilitzsch, Phys. Lett. **B218**, 365 (1989); P. Vogel, G. Schenter, F. Mann and R. Schenter, Phys. Rev. **C24**, 1543 (1981).
- [32] J. Shirai, talk at *ICHEP2000*, XXXth International Conference on High Energy Physics, Osaka, Japan, July 2000.
- [33] R. Barbieri and A. Strumia, hep-ph/0011307.
- [34] V. Barger, S. Geer, R. Raja and K. Whisnant, MADPH-00-1199.
- [35] Proceedings of *Joint U.S. / Japan Workshop On New Initiatives in Muon Lepton Flavor Violation and Neutrino Oscillation with High Intense Muon and Neutrino Sources*, Honolulu, Hawaii, October 2000. http://meco.ps.uci.edu/lepton_workshop/index.html

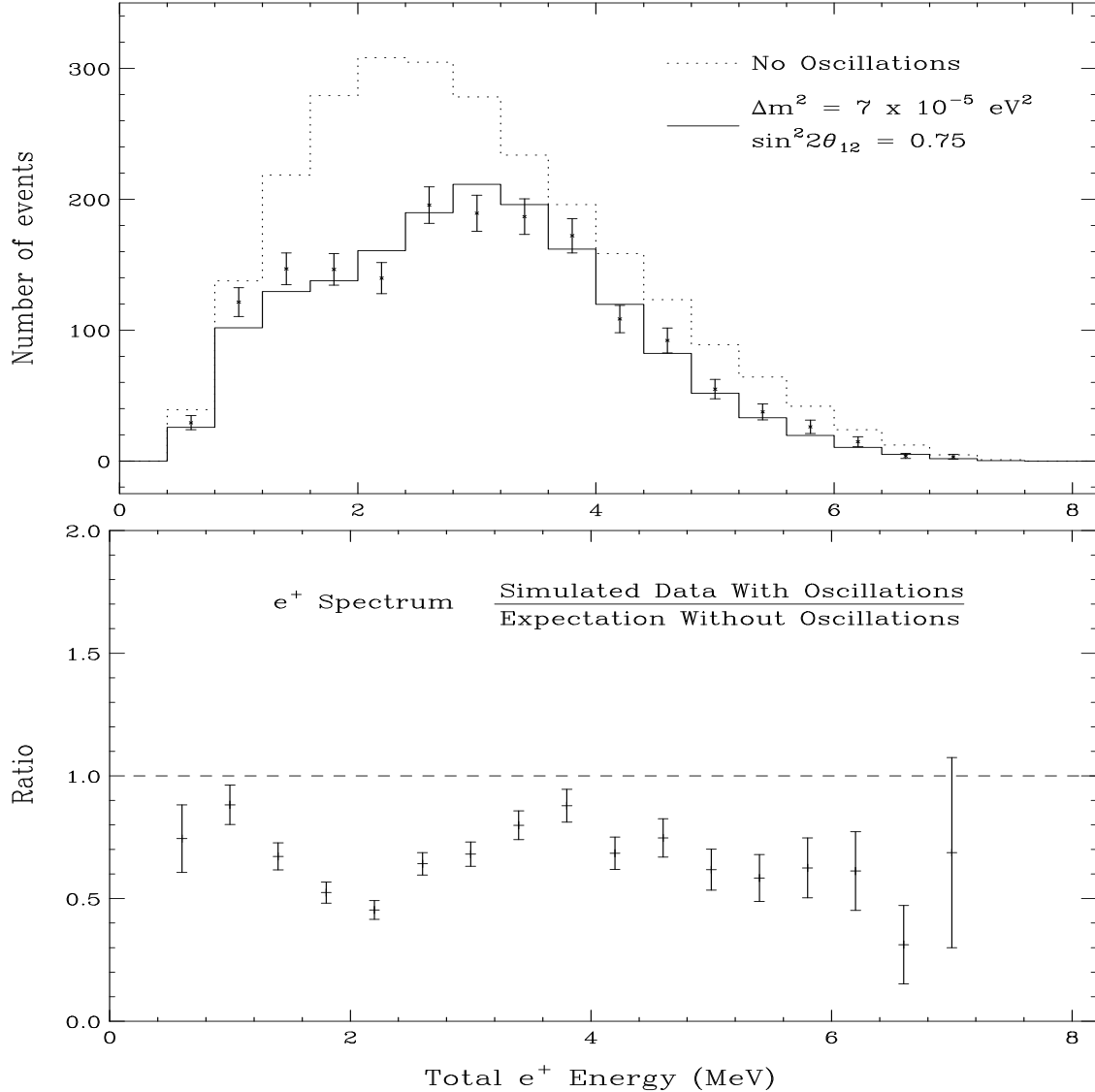


FIG. 1. The expected e^+ energy spectrum (versus total e^+ energy) with three years of accumulated data for the case of no oscillations (dotted histogram) and for $(\Delta m^2, \sin^2 2\theta_{12}) = (7 \times 10^{-5} \text{ eV}^2, 0.75)$ (solid histogram). The data points represent the simulated spectrum. The lower plot shows the ratio of the simulated data to the expectation for no oscillations. The errors shown are statistical.

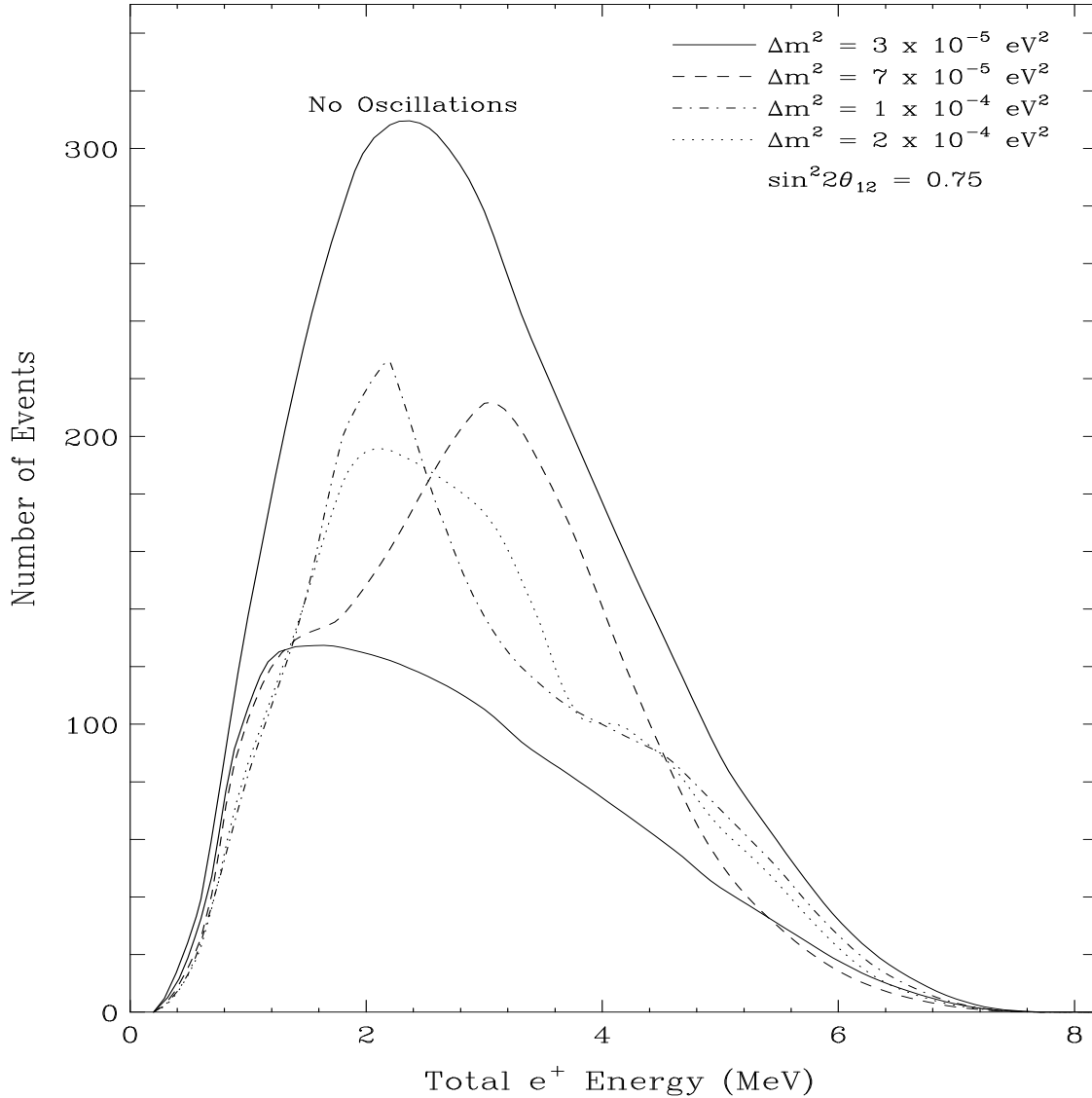


FIG. 2. KamLAND's sensitivity to Δm^2 is unprecedented. In three years it will easily be able to discriminate between only slightly different values of Δm^2 in the LMA region. For $\Delta m^2 \gtrsim 2 \times 10^{-4} \text{ eV}^2$ the spectra overlap significantly.

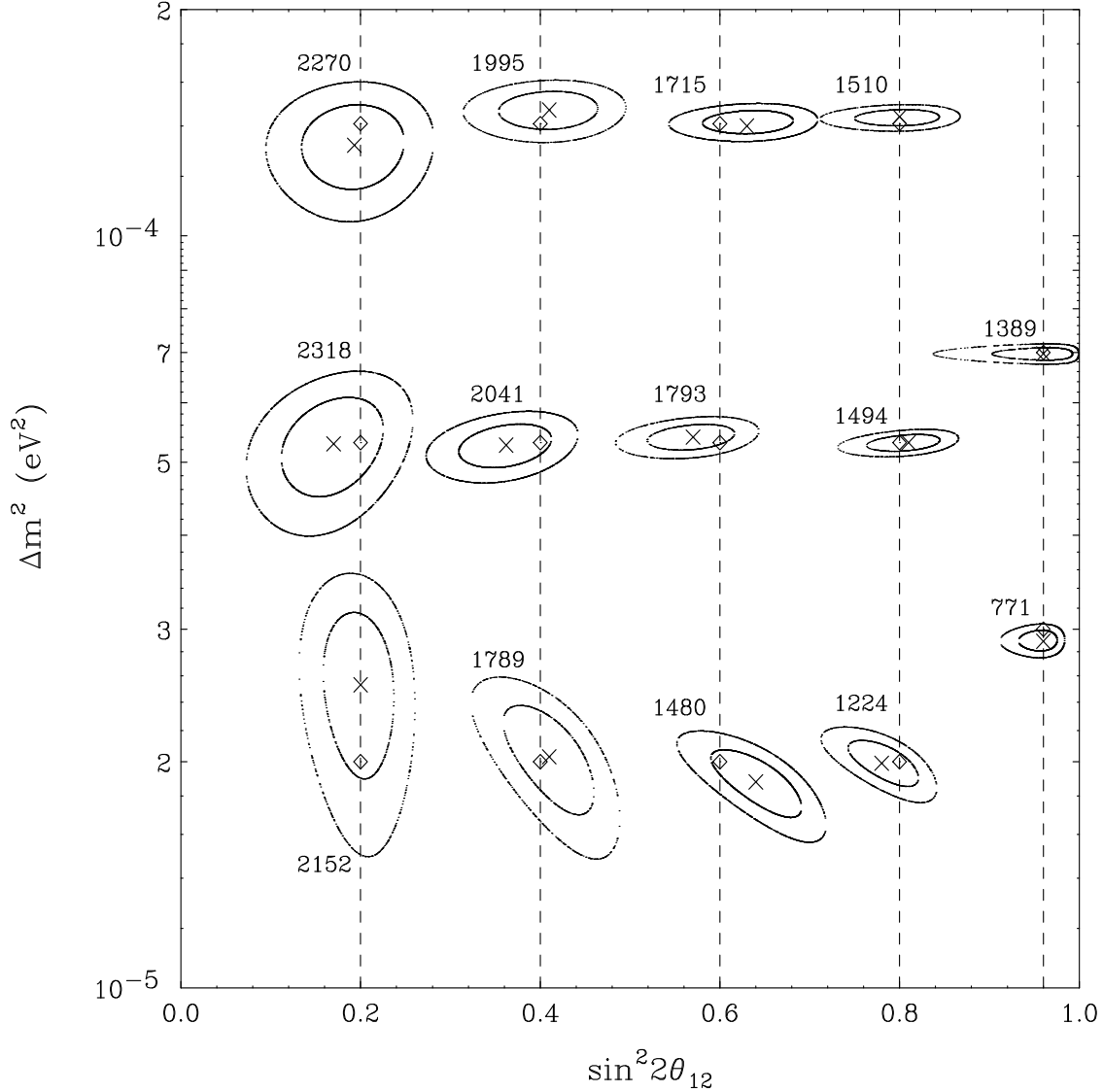


FIG. 3. Fits to e^+ spectra for values of Δm^2 and $\sin^2 2\theta_{12}$ covering the entire region of the LMA solution with $\theta_{13} = 0$. The 1σ (68.3%) and 2σ (95.4%) confidence contours are shown. The diamond is the theoretical value for which data was simulated and the cross marks the best fit point. Each point is labelled by the expected number of signal events in three years. If no oscillations occur, the expectation is 2400 events.

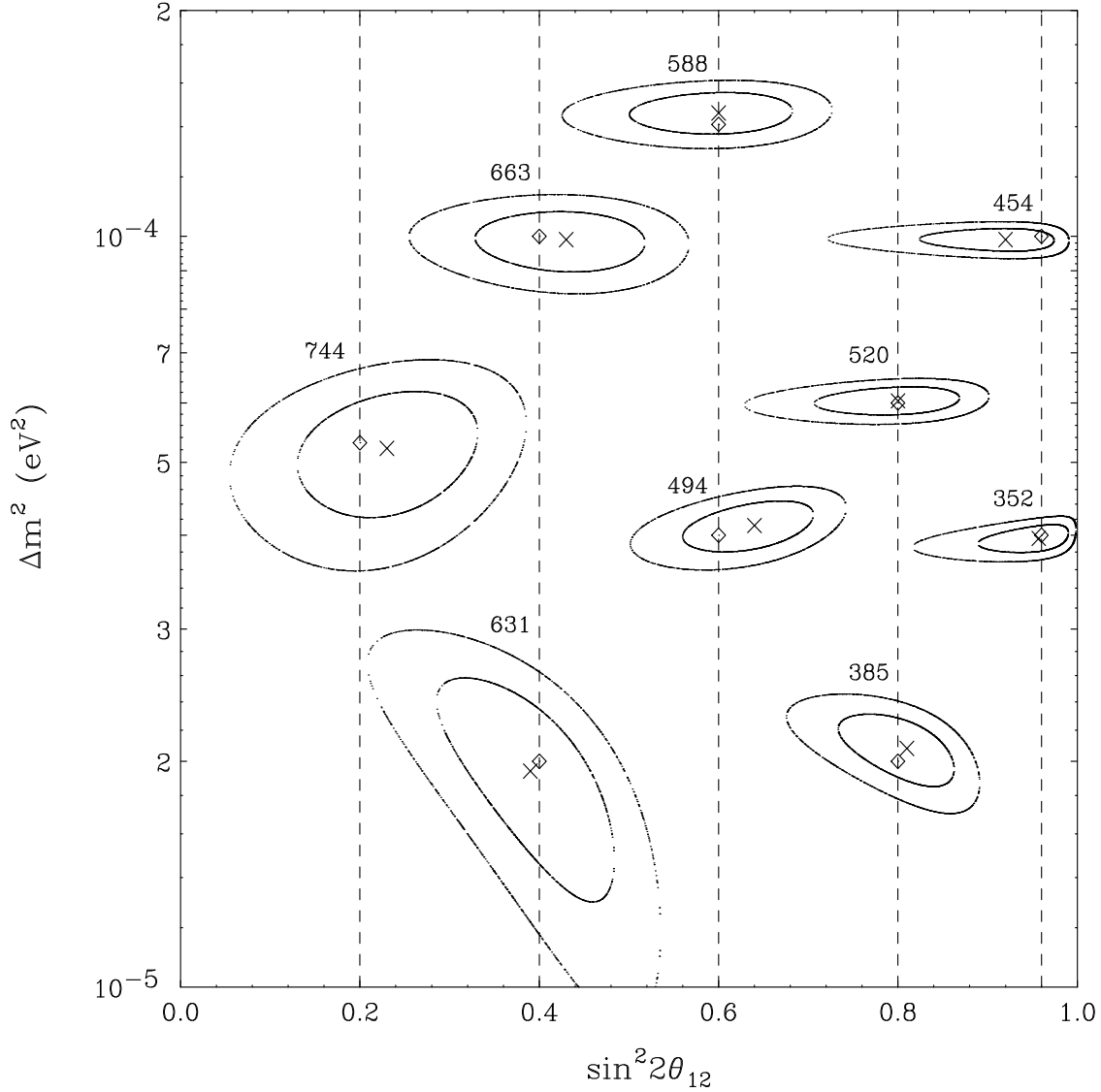


FIG. 4. The same as Fig. 3 except that only one year of accumulated data is assumed. Correspondingly, each point is labelled by the expected number of signal events in one year. If no oscillations occur, the expectation is 800 events.